

Neutral meson and direct photon measurements with the ALICE experiment

Oleksandr Kovalenko

National Centre for Nuclear Research, Warsaw, Poland

December 4, 2019

ALICE group

A. Deloff, P. Kurashvili, O. Kovalenko, T. Marszał, R. Nair, K. Redlich, T. Siemianczuk, G. Wilk

Activities:

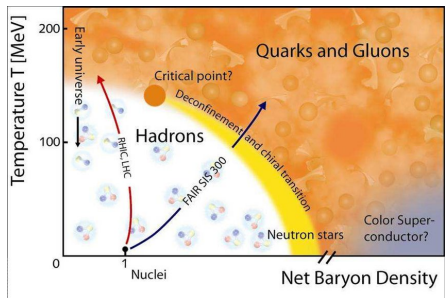
- Upgrade of the PHOS photon spectrometer: extension of the photon energy measurement to 250 GeV (mechanical work, procurement of the front-end electronics (FEE cards) that can handle 50 kHz PbPb and 2 MHz pp collisions, calibration etc).
- Participation in building of the new ALICE fast trigger detector (FIT): procurement of the photosensors, simulations, tests etc.
- Photon, π^0 and η production in pp pPb, XeXe and PbPb collisions.
- Charged particle production in PbPb collisions.

Outline

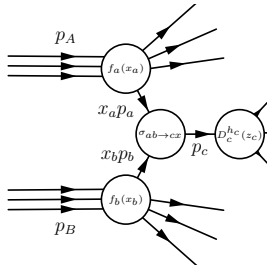
- Introduction
- ALICE setup
- Neutral mesons
 - Measurement techniques
 - pp, p-Pb, Pb-Pb spectra
- Direct photons in Pb-Pb
 - Definitions
 - Spectra per centrality bin
- Summary

Introduction

- Study QCD phase diagram
- Investigate properties of hot ($T \sim 10^{12}$ K) and dense nuclear matter
- Chiral symmetry restoration and the deconfinement (transition from quark to hadronic matter) mechanisms
- Study of the QGP properties



Why hadron spectrometry



Factorization framework:

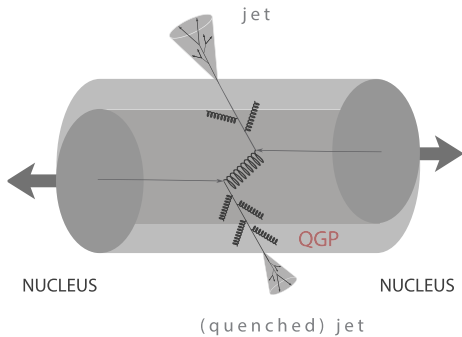
$$d\sigma^{AB \rightarrow h_C X} = f_a(x_a, \mu^2) \otimes f_b(x_b, \mu^2) \otimes d\hat{\sigma}_{ab \rightarrow cx} \otimes D_c^{hc}(z_c, \mu^2)$$

where x_i – momentum fraction carried by a parton, f_i – parton distribution functions, D_c^{hc} – fragmentation function

Why neutral mesons

Meson production in pp should be described by pQCD at large transverse momentum

- Constrain model parameters of perturbative (NLO, NNLO) and non-perturbative regimes (parton distribution function, fragmentation function)
- Test scaling laws
- Main input for direct photon analysis
- Can be identified in a wider p_T range than charged mesons



Direct photons

Inclusive photons

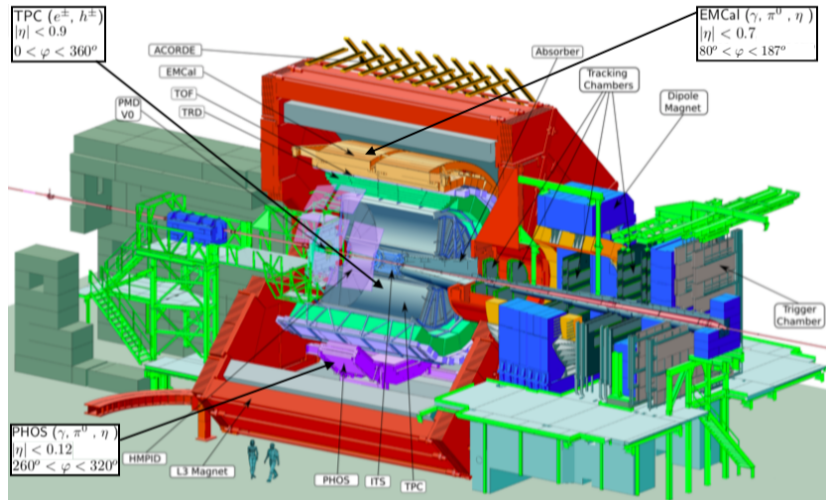
- Decay photons
 - Decay photons coming from π^0 , η , ω , etc.
 - The largest contribution
- Prompt photons
 - Produced in hard scatterings of quark and gluons
 - Mostly contribute at high transverse momentum $p_T \gtrsim 5 \text{ GeV}/c$
- Thermal photons
 - Comes from the collision volume
 - Dominates at $p_T \lesssim 3 \text{ GeV}/c$

Why do we study direct photons?

- Temperature estimation via measurement of p_T distribution of thermal photons in Pb-Pb
- Study of the properties of quark-gluon matter
- Direct photons are produced at all stages of the collisions providing an integrated image of the system

ALICE experiment

Detectors for neutral meson reconstruction

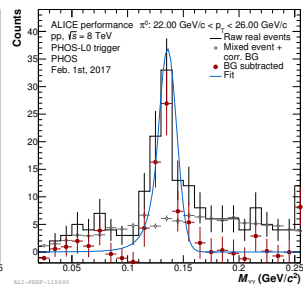
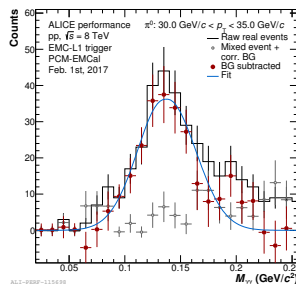
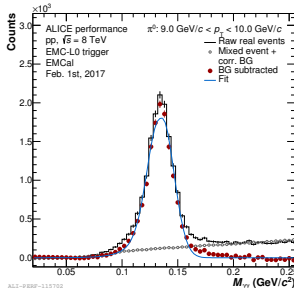


Neutral meson analysis

The neutral mesons can be reconstructed by means of invariant mass analysis

$$M_{\gamma\gamma} = \sqrt{2E_1 E_2 (1 - \cos \theta_{1,2})}$$

- Two gamma channel: hadron $\rightarrow \gamma\gamma$
- Photon conversion (PCM): meson $\rightarrow (\gamma \rightarrow e^+e^-) + (\gamma \rightarrow e^+e^-)$
- Hybrid methods (EMCal + PCM, PHOS + PCM)



Neutral meson analysis

ALICE is able to measure neutral mesons

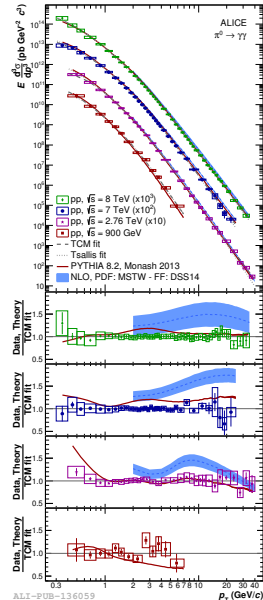
- In different systems (pp, p-Pb, Pb-Pb)
- At different collision energies
- Using different methods
- In the wide p_T range

The measurements from different methods can be combined giving the wide p_T -range of the final spectra

	system	energy
Neutral mesons	pp	0.9, 7 TeV
	pp	2.76 TeV
	pp	8 TeV
	p-Pb	5.02 TeV
	Pb-Pb	2.76 TeV
Direct Photons	pp	2.76, 8 TeV
	Pb-Pb	2.76 TeV

π^0 spectra in pp

- π^0 spectra are up to 40 GeV/c for $\sqrt{s} = 2.76 \text{ TeV}$
- Data shows power law behaviour at high p_T
- PYTHIA 8.2 Monash 2013 describes the data at high p_T
- PYTHIA 8.2 Monash 2013 shows a deviation from the data at moderate p_T at higher energies
- NLO calculations predict 20%-60% higher yield, and the difference increases with p_T

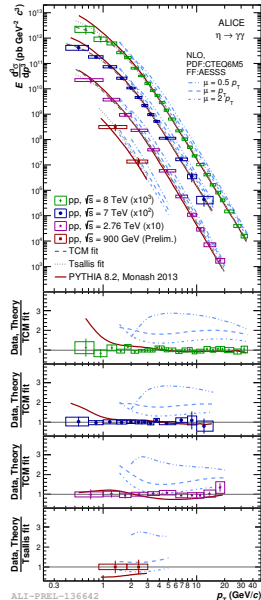


ALI-PUB-136059

10/25

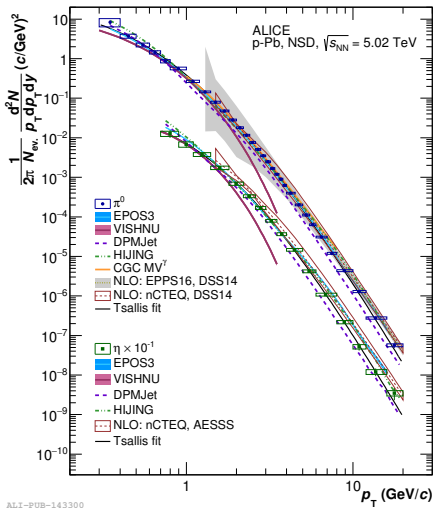
η spectra in pp

- η spectra are up to 40 GeV/c for $\sqrt{s} = 8 \text{ TeV}$
- Data follows power law behaviour at high p_T
- PYTHIA 8.2 Monash 2013 shows a deviation from the data at low p_T at higher energies
- NLO calculations predict 50%-100% higher yield, and the difference increases with p_T



Neutral meson production in p-Pb

- Both π^0 and η spectra are measured up to $p_T < 20 \text{ GeV}/c$
- Various methods for π^0 measurement (PHOS, EMCAL, PCM, PCM-EMCAL)
- EMCAL, PCM, PCM-EMCAL measurements for η production
- Well described by Tsallis function



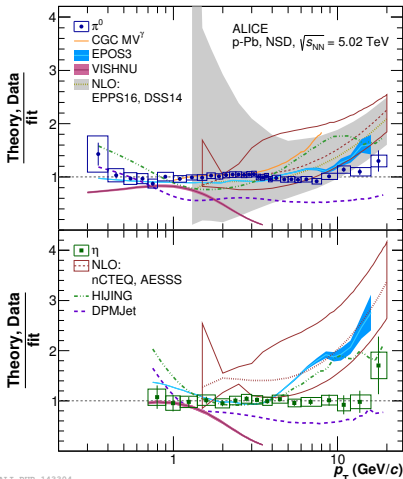
Neutral mesons in p-Pb (comparison with models)

- EPOS3 well reproduces π^0 spectrum
- Problems with η at high p_T (good description below 3 GeV/c)
- VISHNU shows good description at low p_T
- HIJING and DPMJET depart from the data for p_T larger than 4 GeV/c, the disagreement increases with p_T

Related papers:

EPOS3: K.Werner et al., PRC 89
(2014) 064903

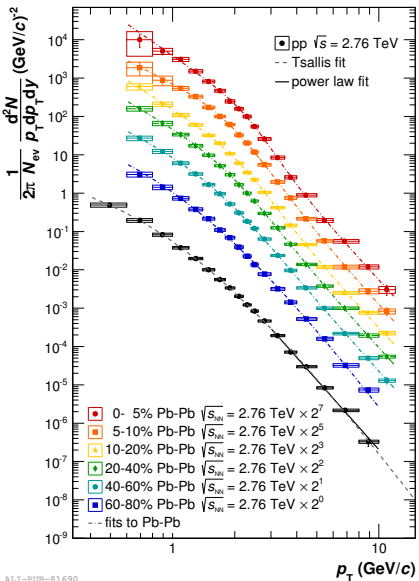
VISHNU: C.Shen et al., PRC 95
(2017) 014906



ALICE-PUB-143304

Neutral pion measurements in Pb-Pb

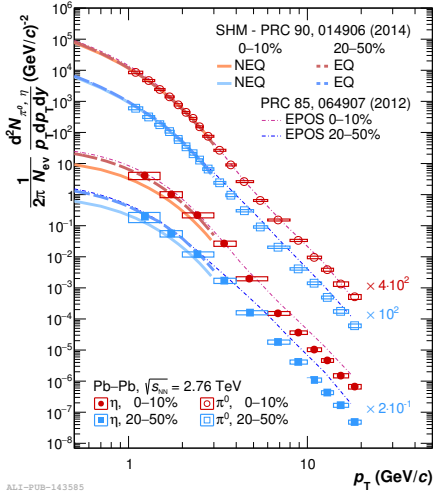
- Based on 2010 data sample
- First measurement of π^0 spectrum in Pb-Pb
 $0.6 < p_T < 12 \text{ GeV}/c$
- Pb-Pb data can be well described by the Tsallis fits
- pp data at $\sqrt{s} = 2.76 \text{ GeV}$ fitted with power law function at high p_T



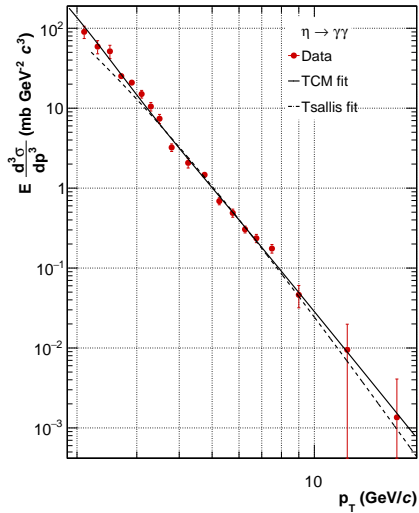
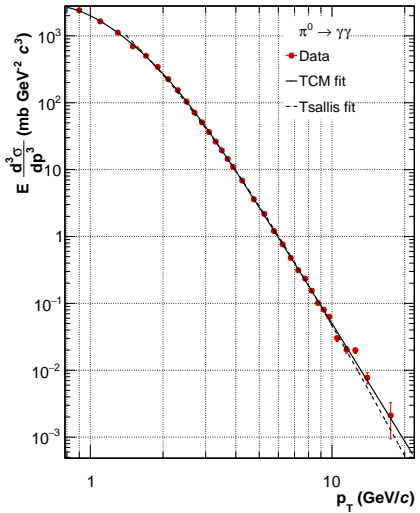
ALICE-PUBLIC-81690

η meson spectra in Pb-Pb

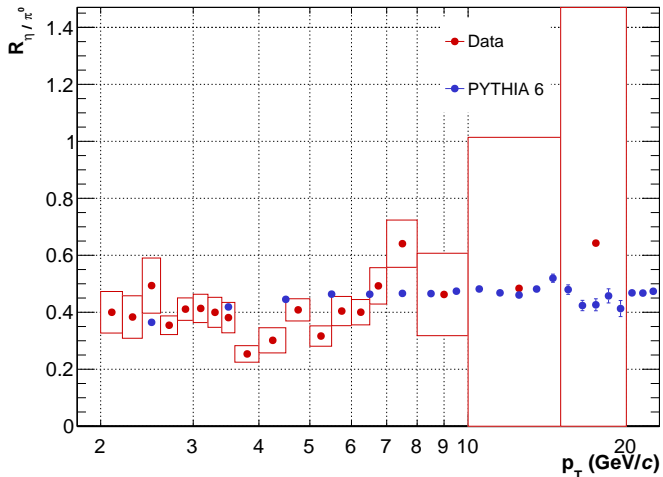
- Increased statistics with 2011 data sample
- First result on η meson spectra in Pb-Pb at the LHC
- The π^0 spectrum extended up to 20 GeV/ c
- Good description of the low p_T region
- The EQ and NEQ versions of SHM reproduce the shape π^0 spectrum at low p_T
- For η NEQ SHM underestimates the yield at the low p_T region



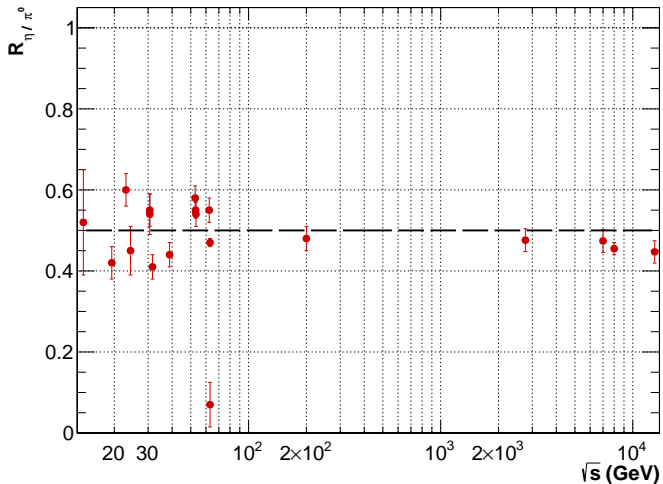
Neutral meson measurements in pp at 13 TeV



η/π^0 spectrum ratio in pp at 13 TeV



η/π^0 at different energies

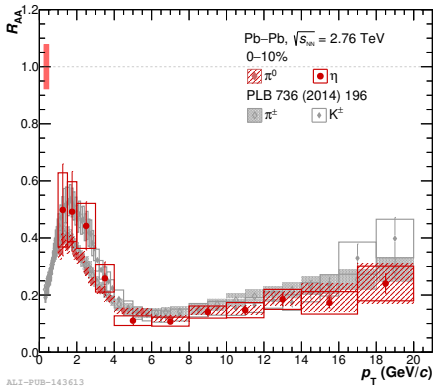


Nuclear modification factor

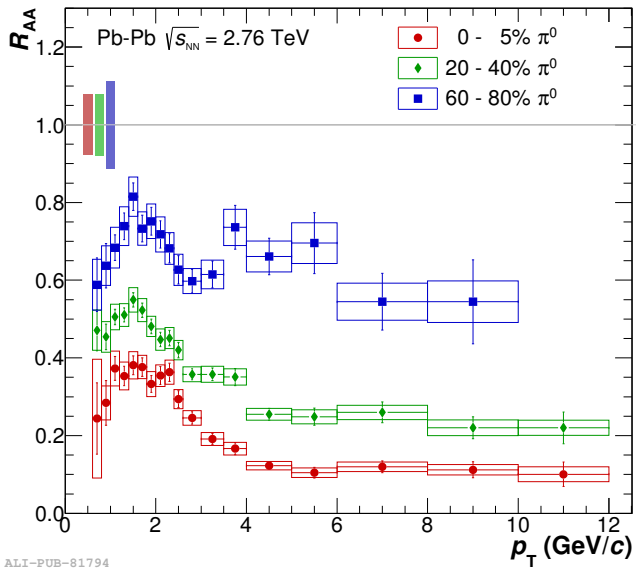
$$R_{AA} = \frac{d^2 N_{AA}/dp_T dy}{\langle T_{AA} \rangle d^2 \sigma_{pp}/dp_T dy}$$

where $\langle T_{AA} \rangle = \langle N_{coll} \rangle / \sigma_{pp}$

- $R_{AA} = 1$ corresponds to the absence of nuclear medium effects
- Observed large suppression $R_{AA} \sim 0.1$ at 7 GeV/c central events. Ratio increases decreasing centrality
- Agrees with results for charged hadrons
- High p_T particle suppression reflects parton energy loss (jet-quenching)

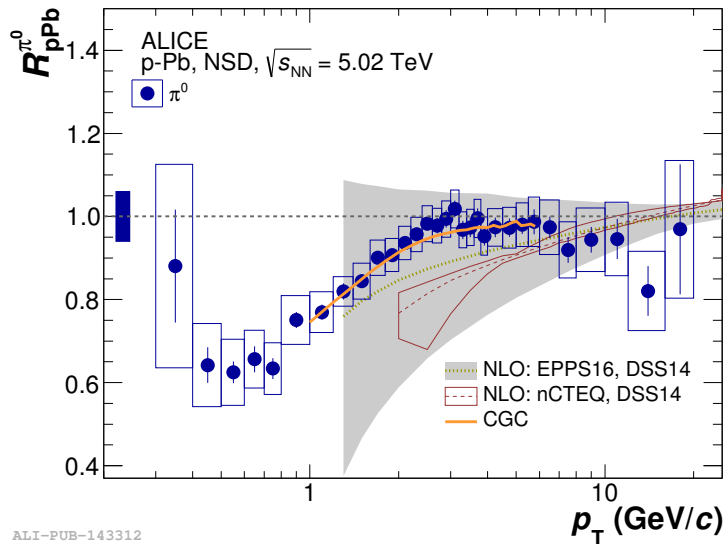


Nuclear modification factor (centrality dependence)



ALI-PUB-81794

Nuclear modification factor p-Pb



ALI-PUB-143312

Direct photon measurements

Direct photons:

All photons that are not coming from hadron decays

$$\gamma_{\text{direct}} = \gamma_{\text{inc}} - \gamma_{\text{decay}} = (1 - 1/R_\gamma) \gamma_{\text{inc}}$$

where $R_\gamma = \gamma_{\text{inc}}/\gamma_{\text{decay}}$

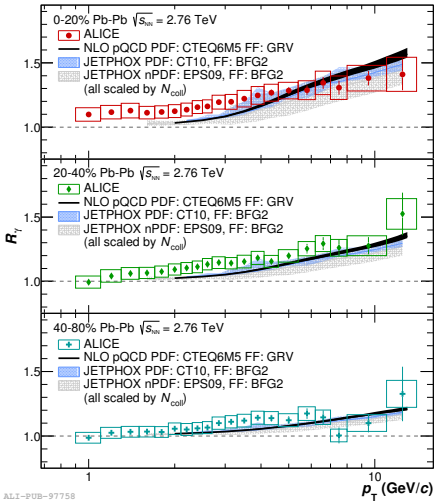
Double Ratio

$$R_{\text{double}} \sim \frac{\gamma_{\text{inc}}/\pi_{\text{par}}^0}{\gamma_{\text{decay}}/\pi_{\text{MC}}^0} \sim R_\gamma$$

Values of R_γ greater than unity indicate the direct photon signal.

Double ratio in Pb-Pb

- Three centrality ranges in $0.9 < p_T < 14 \text{ GeV}/c$
- Compared with JETPHOX and pQCD calculations
- Visible excess of photons (compared to NLO pQCD) at $p_T < 4 \text{ GeV}/c$ in central collisions

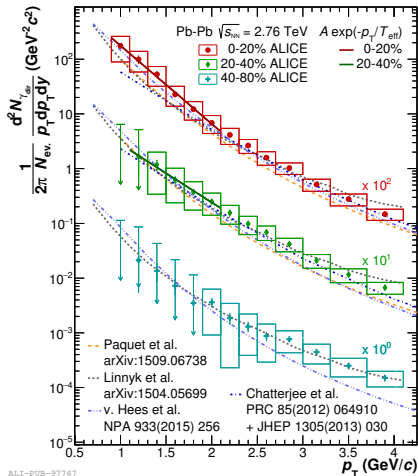


ALI-PUB-97758

Direct photons in Pb-Pb

Different level of agreement for different models, for the central collisions:

- Chatterjee et al.: 2+1 hydro, fluctuating initial conditions, $\tau_0 = 0.14$ fm/c, $\langle T_{\text{init}}^{0-20\%} \rangle = 740$ MeV.
- v. Hees et al.: ideal hydro with initial flow, $\tau_0 = 0.2$ fm/c, $\langle T_{\text{init}}^{0-20\%} \rangle = 682$ MeV,
- Paquet et al.: 2+1 viscous hydro with IP-GLASMA initial conditions, $\tau_0 = 0.14$ fm/c, $\langle T_{\text{init}}^{0-20\%} \rangle = 385$ MeV,
- Linnyk et al.: off-shell transport, microscopic description of evolution,
- Exponential fit for $p_T < 2.2$ GeV/c inv. slope $T_{\text{eff}} = 304 \pm 11$ stat ± 40 sys MeV, which is an estimate of real collision energy, but it doesn't take into account the expanding medium



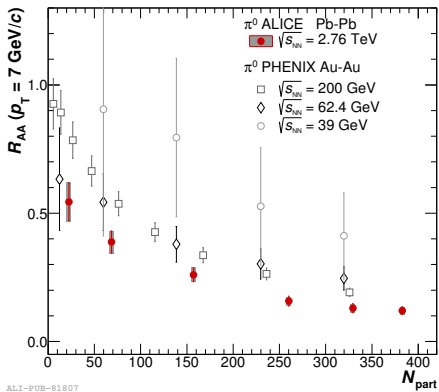
Summary

- ALICE has measured neutral mesons in a wide p_T range
- The measurements allow testing of the parton distribution and fragmentation functions
- The double ratio ($R_\gamma > 1$) in central Pb-Pb collisions exceeds the prompt photon pQCD predictions below 4 GeV/ c
- Various models with QGP formation show different levels of agreement with the measurement
- The inverse slope of direct photon spectrum in central Pb-Pb collisions is ~ 300 MeV

backup slides

Nuclear modification factor, energy dependence

- Clear centrality dependence
- Central collisions lead to more significant effects
- Modification factor decreases with energy (more medium effects at higher energies)



PHOS

- Modular detector
- Consists of $4 \times 64 \times 56$ PbWO_4 crystals
- Crystal size $2.2 \text{ cm} \times 2.2 \text{ cm} \times 18 \text{ cm}$
- Acceptance: $250^\circ < \varphi < 320^\circ$, $|\eta| < 0.13$
- 4.6 m to the interaction point

EMCal and DCal

- 76 layers of scintillator detector, 20 supermodules
- Channel size $6 \text{ cm} \times 6 \text{ cm} \times 24.6 \text{ cm}$
- Acceptance (EMCal): $80^\circ < \varphi < 187^\circ$, $|\eta| < 0.7$
- Acceptance (DCal):
 $260^\circ < \varphi < 320^\circ$, $0.22 < |\eta| < 0.7$,
 $320^\circ < \varphi < 327^\circ$, $\eta < 0.7$
- 4.28 m to the interaction point

Tracking system

Time projection chamber (TPC)

- Barrel shape, with $d = 5 \text{ m}$, $r = 5 \text{ m}$
- Acceptance: $(0 < \varphi < 2\pi, |\eta| < 0.9)$
- Readout chambers 72
- Electrode 100 kV

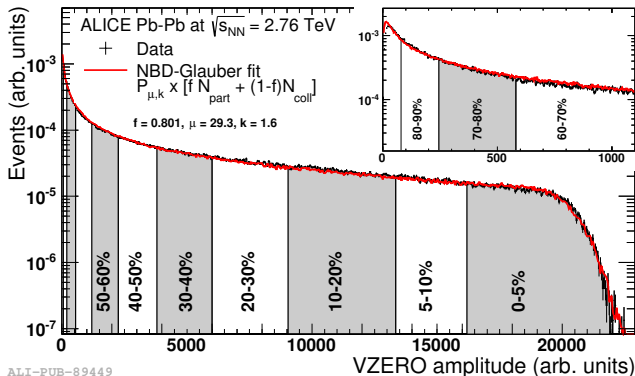
Inner tracking system (ITS)

- 2 layers of pixel detectors (SPD)
- 2 layers of drift detectors (SDD)
- 2 layers of strip detectors (SSD)
- Acceptance: $0 < \varphi < 2\pi, |\eta| < 0.9$

Centrality in Pb-Pb

Centrality classes are defined based on the fractions of Pb-Pb cross-section:

- Charged particle multiplicity in VZERO detector
- Energy deposited in Forward calorimeter ZDC
- Glauber MC, makes correspondence between impact parameter b , and number of binary collision N_{coll} and number of participants N_{part}
- Particle multiplicity per independent source of particles ("ancestors") is modelled by NBD



Functions

Tsallis:

$$E \frac{d^3\sigma^{pp \rightarrow \pi^0 + X}}{dp^3} \sim \frac{\sigma_{pp}^{\text{INEL}}}{2\pi} A \frac{(n-1)(n-2)}{nC(nC + m(n-2))} \left(1 + \frac{m_T - m}{nC}\right)^{-n}$$

Hagedorn:

$$E \frac{d^3\sigma^{pp \rightarrow \pi^0 + X}}{dp^3} \sim \left(\frac{p_0}{p_0 - p_T}\right)^n$$

Power law:

$$E \frac{d^3\sigma^{pp \rightarrow \pi^0 + X}}{dp^3} \sim C p_T^{-n}$$

Two component model:

$$E \frac{d^3\sigma^{pp \rightarrow \pi^0 + X}}{dp^3} \sim A_c \exp(E_{T,\text{kin}}/T_e) + A \left(1 + \frac{p_T^2}{nT^2}\right)^{-n}$$

Decay photon contributions

